

A Singular Role of I_{K1} Promoting the Development of Cardiac Automaticity during Cardiomyocyte Differentiation by I_{K1} -Induced Activation of Pacemaker Current

Yu Sun¹ · Valeriy Timofeyev² · Adrienne Dennis¹ · Emre Bektik^{1,3} · Xiaoping Wan¹ · Kenneth R. Laurita¹ · Isabelle Deschênes¹ · Ronald A. Li^{4,5} · Ji-Dong Fu¹ 

© Springer Science+Business Media New York 2017

Abstract The inward rectifier potassium current (I_{K1}) is generally thought to suppress cardiac automaticity by hyperpolarizing membrane potential (MP). We recently observed that I_{K1} could promote the spontaneously-firing automaticity induced by upregulation of pacemaker funny current (I_f) in adult ventricular cardiomyocytes (CMs). However, the intriguing ability of I_{K1} to activate I_f and thereby promote automaticity has not been explored. In this study, we combined mathematical and experimental assays and found that only I_{K1} and I_f at a proper-ratio of densities, were sufficient to generate rhythmic MP-oscillations even in unexcitable cells (i.e. HEK293T cells and undifferentiated mouse embryonic stem cells [ESCs]). We

termed this effect I_{K1} -induced I_f activation. Consistent with previous findings, our electrophysiological recordings observed that around 50% of mouse (m) and human (h) ESC-differentiated CMs could spontaneously fire action potentials (APs). We found that spontaneously-firing ESC-CMs displayed more hyperpolarized maximum diastolic potential and more outward I_{K1} current than quiescent-yet-excitable m/hESC-CMs. Rather than classical depolarization pacing, quiescent mESC-CMs were able to fire APs spontaneously with an electrode-injected small outward-current that hyperpolarizes MP. The automaticity to spontaneously fire APs was also promoted in quiescent hESC-CMs by an I_{K1} -specific agonist zacopride. In addition, we found that the number of spontaneously-firing m/hESC-CMs was significantly decreased when I_f was acutely upregulated by Ad-CGI-HCN infection. Our study reveals a novel role of I_{K1} promoting the development of cardiac automaticity in m/hESC-CMs through a mechanism of I_{K1} -induced I_f activation and demonstrates a synergistic interaction between I_{K1} and I_f that regulates cardiac automaticity.

Yu Sun and Valeriy Timofeyev contributed equally to this study.

Electronic supplementary material The online version of this article (doi:10.1007/s12015-017-9745-1) contains supplementary material, which is available to authorized users.

✉ Ronald A. Li
ronaldli@hku.hk

✉ Ji-Dong Fu
jidadong.fu@case.edu

¹ Department of Medicine, Heart and Vascular Research Center, MetroHealth Campus, Case Western Reserve University, 2500 Metrohealth Drive, Rammelkamp 650, Cleveland, OH 44109, USA

² Department of Internal Medicine, University of California, Davis, CA, USA

³ Ph.D. Program in Human Biology, School of Integrative and Global Majors, University of Tsukuba, Tsukuba, Japan

⁴ Dr. Li Dak-Sum Center for Regenerative Medicine, University of Hong Kong, The Hong Kong Jockey Club Building for Interdisciplinary Research, LB 5-065 Sassoon Road, Pokfulam, Hong Kong

⁵ Ming-Wai Lau Center for Regenerative Medicine, Karolinska Institutet, Solna, Sweden

Keywords I_{K1} · I_f · Rhythmic oscillation · Automaticity · Embryonic stem cell · Cardiomyocyte differentiation

Introduction

Cardiac automaticity refers to spontaneously generated electrical impulses (i.e., action potentials). In the adult heart, it is pacemaker cells in the sinoatrial node that are dedicated to generate impulses to maintain the heart's rhythmic beating; however, in the fetal heart, all cardiomyocytes (CMs), including ventricular and atrial CMs, have high automaticity and are able to spontaneously fire action potentials (APs) [1]. It is still poorly understood how cardiac automaticity is developed

during CM differentiation. Cardiac automaticity is the result of an ensemble of ion currents through sarcolemmal ion channels [2, 3]. Among those ion currents, a pacemaker “funny” current (I_f), encoded by the hyperpolarization-activated, cyclic-nucleotide gated (HCN)-family of genes [4], is responsible for initiating the diastolic depolarization and determines the rate of spontaneous pacemaker activity [5–7]. Overexpression of HCN channels in neonatal ventricular myocytes increases the beating frequency [8], and injection of adenovirus-HCN into the left atrium *in vivo* induces ectopic pacemaking foci [9, 10]. In contrast, the inward rectifier potassium current (I_{K1}) has been generally thought to play an inhibitory role in the induction of cardiac automaticity [2, 3].

I_{K1} , encoded by Kir2.x genes [11], contains both inward (depolarizing) and outward (hyperpolarizing) current components; the outward component stabilizes the resting membrane potential (RMP) and contributes to the phase-3 repolarization of APs [12–14]. I_{K1} is abundant in the working myocardium of the atrium and ventricle but is low [15, 16] or non-measurable [17] in pacemaker cells of the sinoatrial node. As a stabilizer, I_{K1} is generally recognized to suppress cardiac automaticity. In a transgenic mouse model, Kir2.1 knockout prolongs the AP duration (APD) and increases the number of ventricular CMs that can spontaneously fire APs [18]. Andersen-Tawil syndrome in humans with episodic cardiac arrhythmias and developmental dysmorphic features are also caused by mutations in Kir2.1 [14, 19]. It has been observed that the low amount of I_{K1} and high amount of I_f contribute to the high automaticity of fetal CMs [1, 20, 21] as well as CMs differentiated from mouse (m) and human (h) embryonic stem cells (ESCs) [22–24], which have been broadly used to understand mouse and human developmental biology and embryogenesis, including cardiogenesis of pacemaker cells and atrial and ventricular CMs [22–28]. Our previous study found that overexpression of Kir2.1 facilitates the electrophysiological maturation of m/hESC-differentiated CMs by converting spontaneously AP-firing cells into quiescent-yet-excitabile electrophysiological-matured CMs [23]. Meanwhile, the strategy of suppressing I_{K1} has also been exploited to develop bioengineered pacemakers. Knocking-down Kir2.1 channels in adult ventricular CMs resulted in a depolarization of RMP and induced endogenous pacemaker activity [14, 29], a similar result of developing bio-pacemaker cells from ventricular CMs by overexpression of HCN channels [9, 10]. Interestingly, our studies observed that co-overexpression of Kir2.1 with engineered-HCN1 could further enhance the induced automaticity of ventricular CMs to spontaneously fire APs at a faster rate [30]. Given that I_f is activated by hyperpolarization, however, the intriguing ability of I_{K1} to activate I_f and thereby promote automaticity has not been explored.

In the present study, we first applied a computational mathematical-modeling assay to investigate the synergistic interaction between I_{K1} and I_f and found that a combination

of I_{K1} and I_f was sufficient to induce rhythmic oscillation of membrane potential (MP), which was experimentally replicated in unexcitable HEK293T cells and undifferentiated mouse ESCs. Our electrophysiological study revealed a novel unexpected role of I_{K1} in promoting the induction of cardiac automaticity in m/hESC-CMs during cardiac differentiation. We also found that acute upregulation of I_f induced by infection of Ad-CGI-HCN virus inhibited the automaticity of m/hESC-CMs, which is surprisingly different from an increased automaticity of CMs differentiated from a stable HCN4-transgenic mESCs [31], but is consistent with our mathematical-modeling assay.

Materials and Methods

Differentiation and Isolation of Mouse and Human ESC-CMs

D3 cell line of mouse ESCs (ATCC) were cultivated and differentiated into spontaneously-beating CMs by embryoid body (EB)-mediated differentiation [32]. The hES2 human ESCs (ES Cell International [ESI], Singapore) were maintained as previously reported [33]. The hES2 cells were differentiated into CMs by co-culturing with the immortalized endoderm-like END2 cells [26]. To isolate single CMs, beating outgrowths were microscurgically dissected from differentiated hESCs (Day 16 ~ 20) and mouse EBs (Day 7 + 4) by a glass knife, followed by incubating in collagenase solution (1 mg/ml) at 37 °C for 30 min [22, 27, 32]. The isolated cells were incubated with KB solution containing (mmol/L): 85 KCl, 30 K_2HPO_4 , 5 $MgSO_4$, 1 EGTA, 2 Na_2-ATP , 5 pyruvic acid, 5 creatine, 20 taurine, and 20 D-glucose, at room temperature for 30 min. After the cells were plated on laminin-coated glass coverslips for 1 h at 37 °C, the culture media was added carefully and refreshed the next day.

Lentivirus- and Adenovirus-Mediated Gene Transfer

Fusion protein of human HCN4GFP or Kir2.1dsRed was inserted into the pLV-EF1 α -GFP plasmid to replace GFP at the Pac I and Nde I restriction sites; these two lentiviral plasmids were used to mediate the upregulation of I_{K1} and I_f , respectively. The recombinant lentiviruses were produced by transient transfection of HEK293T cells as previously described [22, 24]. Briefly, the lentiviral plasmids p Δ 8.91, pMD.G, and pLV-EF1 α -gene vector (2:1:3 mass ratio) were co-transfected into HEK293T cells. The supernatants that contain lentiviral particles were harvested at 24- and 48-h post-transfection and stored at -80 °C before use. In the presence of polybrene (6 μ g/ml), lentiviral particles with a $> 10^6$ titer infected cells with a multiplicity of infection of 3. The

fluorescence of GFP or dsRed was used to select positively-transduced cells.

An adenovirus vector of pAd-CMV-GFP-IRES (Ad-CGI) with bioengineered mouse HCN1 (pAd-CGI-HCN) was used to mediate the overexpression of I_f in m/hESC-CMs as in our previous study [10, 23, 34]. The empty adenovirus was used as the control. Adenoviruses were generated by Cre-lox recombination of purified ψ 5 viral DNA and shuttle vector DNA. The recombinant products were plaque-purified, expanded, and concentrated by CsCl gradient, yielding concentrations of 10^{10} plaque formation unit (PFU)/ml. For transduction, adenoviral particles were added at a concentration of $\sim 2 \times 10^9$ PFU [10]. Adenoviral-infected cells were used for electrophysiological characterization within two to four days after adenoviral infection.

Electrophysiological Characterization

Electrophysiological experiments were performed at the single cell level by whole-cell patch-clamp with an Axopatch 200B amplifier and the pClamp10.2 software (Axon Instruments Inc., Foster City, CA) [22–24, 35]. Patch pipettes were prepared from 1.5 mm thin-walled borosilicate glass tubes using a Sutter micropipette puller P-97 and had typical resistances of 4–6 M Ω when filled with an internal solution containing (mmol/L): 110 K-aspartate, 20 KCl, 1 MgCl₂, 0.1 Na-GTP, 5 Mg-ATP, 5 Na₂-phosphocreatine, 1 EGTA, 10 HEPES, pH adjusted to 7.3 with KOH. The external Tyrode's bath solution consisted of (mmol/L): 140 NaCl, 5 KCl, 1 CaCl₂, 1 MgCl₂, 10 D-glucose, 10 HEPES, pH adjusted to 7.4 with NaOH. Voltage- and current-clamp recordings were performed at 37 °C. The electrode potential was adjusted to zero after immersion of the pipette tip, which caused a positive voltage bias of measured MPs and was corrected with a junction potential (−14.9 mV).

APs were directly recorded from spontaneously-firing m/hESC-CMs by current-clamp without electrical stimulus and were elicited and recorded in quiescent cells with a stimulus of 0.1–1 nA for 5 ms. Based on the parameters of APs (Table 1), m/hESC-CMs were categorized into pacemaker, atrial, or ventricular phenotypes [23, 36]. In brief, ventricular m/hESC-CMs have longer APD, APD₅₀, and APD₉₀ than atrial cells; a ratio of the duration at different levels of 10% repolarization, APD_{30–40}/APD_{70–80} that indicates “plateau” during phase 2, was used to categorize the cells as atrial (<1.4) or ventricular (≥ 1.4); the maximum depolarization rate (dV/dT_{Max}) of AP was applied to distinguish pacemaker cells (<5 mV/ms) from atrial and ventricular cells.

After AP characterization, I_{K1} and I_f were measured in the same cell by switching current-clamp to voltage-clamp recordings. To measure I_{K1} and I_f , cells were held at a -30 mV potential and pulsed for 2 s from 0 mV to -140 mV with 10 mV increments of every sweep, followed by a -100 mV

pulse for 1 s. I_{K1} was defined as 1 mmol/L Ba²⁺-sensitive currents; I_f was represented by the remaining Ba²⁺-nonsensitive currents.

Single Cell Real Time RT-PCR

Right after patch-clamp recording of APs, some individual hESC-CMs were manually picked up by the recording pipette and transferred into 0.2 ml PCR tubes for reverse transcription (RT) and pre-amplification of cDNA by using CellsDirect One-Step qRT-PCR kit (Invitrogen) together with pooled primers (Supplemental Table 1). The amplified cDNA samples were diluted 20 times and stored in -80 °C. To evaluate the gene expression of individual hESC-CMs, the standard real time PCR was set up as the product manual of SsoFast™ EvaGreen® Supermixe with low ROX (Bio-Rad), and data were collected and analyzed on an ABI-7500 real time PCR system (Applied Biosystems). Ct values were used to indicate the expression of genes. Supplemental Table 1 includes the information of primers.

Immunocytochemistry

Differentiated hESC-CMs (D21) were digested and plated on laminin-coated glass coverslips. Cells were fixed for 15 min at room temperature with methanol-acetone (1:1) mixture. After washing with PBS, cells were incubated with 10% goat serum for 30 min and then incubated with primary rabbit anti-Kir2.1 or anti-HCN4 antibody (Alomone Labs) together with mouse anti- α -actinin monoclonal antibody (Sigma). Alexa Fluor-488 goat anti-mouse IgG and Alexa Fluor-594 goat anti-rabbit IgG (Invitrogen) were used for fluorescence imaging. Coverslips were mounted onto glass slides in Prolong Gold antifade mountant with DAPI (ThermoFisher). Samples were imaged on a confocal laser-scanning microscope (Leica TCS SP8).

Formulation of a Mathematical Model

A mathematical modeling approach was applied to investigate the systematic coordination of I_{K1} and I_f by a well-established mathematical model that was originally established for rabbit SAN pacemaker cells [37]. Rather than nine membrane currents applied in the original model, only I_{K1} and I_f , without other ion currents, were included in our single cell model with their typical kinetics. Time-dependent behavior of two currents is described using gating variables obeying first-order Hodgkin-Huxley kinetics. Our model uses the same initial extracellular and cytosolic ion concentrations as that in the original model [37]. MATLAB 6.5 was used to perform the programming assay. Differential equations were solved using the Euler method. A fixed constant step of integration 0.01 ms was used.

Table 1 Parameters of Action Potential Recorded in Human and Mouse ESC-CMs

Human ESC-CMs	MDP (mV)	APA (mV)	APD ₅₀ (ms)	APD ₉₀ (ms)	APD ₃₀₋₄₀ /APD ₇₀₋₈₀	dV/dT _{Max} (mV/ms)	Firing Rate (fpm)
Control							
Pacemaker (2)	-56.0 ± 3.9	48.3 ± 1.4	30.2 ± 6.0	149.7 ± 7.3	1.0 ± 0.2	4.7 ± 1.0	48.2 ± 2.5
A Firing (4)	-69.5 ± 5.1*	67.8 ± 15.8	67.0 ± 13.6	110.2 ± 24.4	1.0 ± 0.4	35.7 ± 14.6	222.6 ± 76.0
Paced (6)	-57.6 ± 2.6	86.4 ± 6.4	32.4 ± 3.0	113.2 ± 7.1	0.9 ± 0.5	20.6 ± 4.4	
V Firing (9)	-71.1 ± 4.3*	68.1 ± 3.1	276.1 ± 44.3	341.0 ± 46.7	3.0 ± 0.7	15.2 ± 8.4	35.7 ± 6.3
Paced (12)	-64.7 ± 2.7	90.9 ± 4.8	259.6 ± 39.8	370.8 ± 49.9	2.7 ± 0.6	22.4 ± 5.3	
HCN							
Pacemaker (0)							
A Firing (0)							
Paced (12)	-55.4 ± 3.5	83.7 ± 6.1	26.1 ± 5.1	88.3 ± 15.6	0.9 ± 0.4	20.7 ± 1.7	
V Firing (8)	-62.0 ± 3.0*	59.3 ± 5.6	180.5 ± 34.7	230.6 ± 39.9	2.8 ± 0.6	15.8 ± 6.2	34.5 ± 7.0
Paced (8)	-57.5 ± 2.2	80.0 ± 7.4	116.0 ± 25.2	236.3 ± 34.8	2.5 ± 0.6	20.2 ± 1.7	
Mouse ESC-CMs							
Pacemaker (3)	-65.9 ± 0.9	49.2 ± 1.6	42.5 ± 6.8	127.5 ± 41.8	1.0 ± 0.1	3.1 ± 0.8	138.2 ± 69.1
A Firing (13)	-71.5 ± 1.5**	81.7 ± 12.4	27.9 ± 4.6	79.5 ± 9.4	1.0 ± 0.2	38.2 ± 11.8	273.0 ± 44.1
Paced (19)	-64.8 ± 2.1	108.9 ± 7.7	20.8 ± 2.8	51.8 ± 5.2	0.9 ± 0.1	28.9 ± 3.4	
V Firing (12)	-72.4 ± 3.1*	84.6 ± 6.7	74.7 ± 11.8	123.8 ± 20.7	1.8 ± 0.4	34.7 ± 13.8	175.7 ± 40.5
Paced (13)	-67.5 ± 3.2	107.5 ± 6.4	66.6 ± 11.8	129.2 ± 10.7	1.9 ± 0.3	34.6 ± 8.6	
Pacemaker (3)	-66.9 ± 3.1	44.4 ± 7.5	103.9 ± 36.1	172.9 ± 55.9	0.9 ± 0.2	3.3 ± 1.3	110.5 ± 23.6
A Firing (4)	-73.9 ± 2.2*	71.3 ± 10.8	39.1 ± 14.2	66.3 ± 28.3	1.0 ± 0.2	27.0 ± 6.2	207.5 ± 65.4
Paced (35)	-67.4 ± 1.3	108.0 ± 4.7	19.1 ± 1.2	46.4 ± 2.7	0.9 ± 0.2	21.1 ± 1.4	
V Firing (0)							
Paced (27)	-71.1 ± 2.0	107.6 ± 5.3	136.5 ± 30.3	184.3 ± 31.9	2.0 ± 0.3	20.4 ± 1.6	

MDP; maximum diastolic potential; APA, action potential amplitude; APD, action potential duration; APD₅₀ and APD₉₀, AP duration at 50% or 90% repolarization; APD₃₀₋₄₀/APD₇₀₋₈₀, a ratio of the duration at different levels of 10% repolarization which indicates "plateau" during phase 2; dV/dT_{Max}, maximal rate of depolarization; fpm: firing per minute. Values are expressed as mean ± s.e.m.; **p* < 0.05 and ***p* < 0.01, Spontaneously-Firing vs. Quiescent-Paced counterpart.

Statistical Analysis

Data are expressed as mean \pm S.E.M. Statistical significance of differences in means was estimated by unpaired Student's *t* test or Chi-square (χ^2) test. $p < 0.05$ was considered statistically significant.

Results

I_{K1} -Induced I_f Activation Programmed Rhythmic Oscillations in *in Silico* Analysis

Since we recently found that I_{K1} could promote the spontaneously-firing automaticity induced by upregulation of I_f in adult ventricular CMs [30]; we first investigated how I_{K1} and I_f synergistically interact with each other by mathematical simulation. Without any other ionic currents, only I_{K1} and I_f with a typical current-voltage (I-V) relationship (Fig. 1a) were included in a well-established mathematical model that was originally developed for rabbit SAN pacemaker cells [37]. Remarkably, the rhythmic oscillation of MP, a pacemaker-like activity, could be successfully programmed by I_f and I_{K1} (Fig. 1b). The MP was oscillating between -80 mV and -35 mV in our simulation assay. In theory, the outward current of I_{K1} hyperpolarizes MP, which subsequently activates HCN-channels; the inward current of I_f depolarizes MP, which then activates the outward current of I_{K1} to hyperpolarize MP again and to induce rhythmic MP-oscillation (Fig. 1c). We termed this mechanistic model I_{K1} -induced I_f activation. Noticeably, inducing MP oscillation requires a large amount of I_f and a small amount of I_{K1} , meaning that any small-amount of increased I_{K1} will require much more I_f to induce MP oscillation.

We calculated the oscillation rate after a 10-s simulation of I_{K1} and I_f and found that a proper ratio of I_{K1} and I_f was critical for the induction of this MP oscillation and controlled the frequency of rhythmic oscillation (Fig. 1d). A specific level of I_f and I_{K1} at spot "a" in Fig. 1d could induce a 3 Hz oscillation of MP, which was increased to 4.5 Hz with more I_{K1} (spot "b"); however, a further increasing of I_{K1} quickly suppressed the rhythmic oscillation (spot "c"). This result demonstrated that a proper amount of I_{K1} could help I_f to accelerate this rhythmic MP oscillation. Interestingly, too much I_f without a corresponding increase of I_{K1} suppressed the induction of MP oscillation (spot "d" in Fig. 1d).

Generating Rhythmic Oscillations in Unexcitable Cells by I_{K1} -Induced I_f Activation

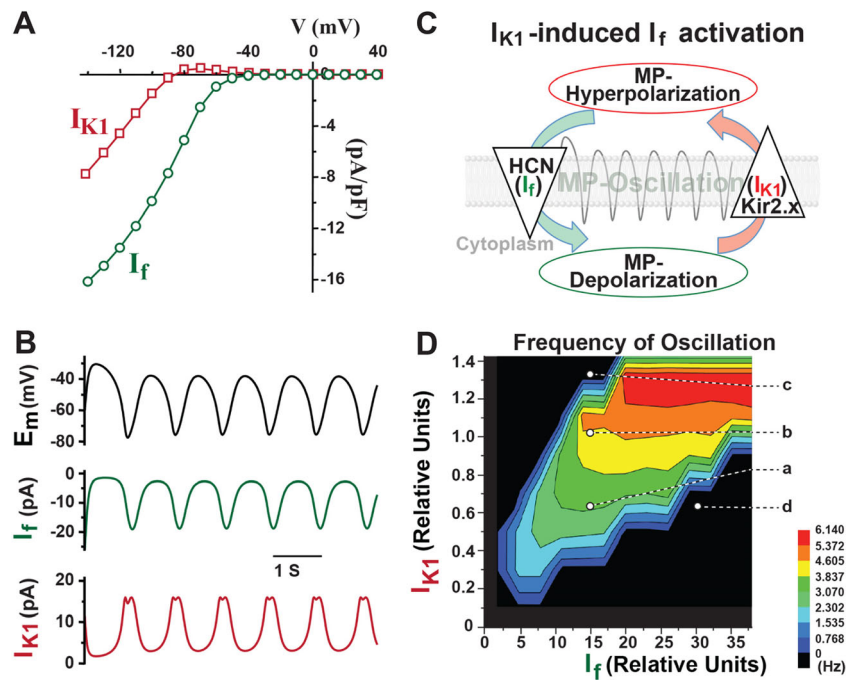
We next investigated if this computational simulation of rhythmic oscillation, driven by I_{K1} -induced I_f activation, happens in a real biological system. We introduced two fusion

proteins—Kir2.1dsRed and HCN4GFP—into unexcitable HEK293T cells by lentiviral transduction (Fig. 2a) and measured a huge I_{K1} with a big outward current (8.0 ± 6.1 pA/pF at -60 mV, $n = 8$) and an intermediate inward current of I_f (-3.7 ± 2.0 pA/pF at -60 mV, $n = 8$) in the Kir2.1dsRed/HCN4GFP-cotransduced cells (Fig. 2b-c). With such a huge I_{K1} , the MP of HEK293T cells that overexpressed Kir2.1 were hyperpolarized to -92.1 ± 0.5 mV ($n = 68$) and -91.1 ± 1.9 mV ($n = 24$) with and without the expression of HCN4 channels, respectively (Fig. 2d), while the MP was much more positive in wild-type (-28.2 ± 1.1 mV, $n = 21$) and HCN4-transduced (-35.3 ± 1.9 mV, $n = 19$) cells.

Remarkably, the MP of HCN4/Kir2.1-co-transduced HEK293T cells was rhythmically oscillating between -85 mV and -35 mV when I_{K1} was partially blocked by Ba^{2+} perfusate (40 μ mol/L, $n = 5$ out of 11) or when the blocked I_{K1} was partially recovered ($n = 8$ out of 11) by washing out Ba^{2+} (Fig. 2e). Neither HEK293T cells that overexpressed Kir2.1 alone nor those that overexpressed HCN4 alone could ignite a rhythmic electrical oscillation (Fig. S1), indicating a unique ying-and-yang interaction between I_{K1} and I_f . Indeed, this pacemaker-like rhythmic electrical activity driven by I_{K1} and I_f could be replicated in undifferentiated mESCs (another unexcitable cell type) (Fig. S2). When Kir2.1dsRed was introduced into mESCs, in which we could record I_f but not I_{K1} [35], its MP became hyperpolarized as anticipated (Fig. S2c). Similarly, spontaneous MP-oscillations between -70 mV to -35 mV were observed in Kir2.1-transduced mESCs ($n = 3$ out of 6) when I_{K1} was partially blocked by Ba^{2+} . Collectively, our experiments demonstrated that the unique synergistic interaction between I_{K1} and I_f is sufficient to program a rhythmic electrical activity in unexcitable cells.

In HCN4/Kir2.1-transduced HEK293T cells, I_{K1} hyperpolarizes MP and I_f is the major inward current for depolarization. Given that I_f is insensitive to millimolar concentrations of external Ba^{2+} [4], I_f would be expected to remain largely unchanged while I_{K1} is modulated by Ba^{2+} (40 μ mol/L) perfusion or wash-out (Fig. 2e). When Ba^{2+} was administered to quiescent HCN4/Kir2.1 HEK293T cells, I_{K1} was decreased gradually, yielding rhythmic oscillations of MP (time point "a" of Fig. 2e); when I_{K1} was further decreased as Ba^{2+} blockade continued, the firing rate decreased (time point "b") until the cells subsequently became quiescent at a MP (< -45 mV) that was no longer hyperpolarized by insufficient outward current of I_{K1} for I_f -activation. Oscillations were restored during Ba^{2+} wash-out when I_{K1} gradually increased back to the suitable range where I_{K1} -activated I_f activation takes place. These experiments successfully replicated our computational assay that a synergistic interaction of I_{K1} and I_f is sufficient to induce rhythmic MP oscillation.

Fig. 1 The in silico simulation shows that I_{K1} -induced I_f activation programs rhythmic oscillations of membrane potential (MP). **a** Representative Current-Voltage (I-V) curves of I_{K1} (red) and I_f (green) were applied in the mathematic model. **b** Only I_{K1} and I_f , without other ion currents, were sufficient to program rhythmic oscillations of MP. **c** A schema illustrates the mechanism of how I_{K1} -induced I_f activation generates rhythmic oscillation of MP. **d** A surface contour shows that the ratio of I_{K1} and I_f regulates the frequency of rhythmic oscillation



I_{K1} Improves the Induction of Cardiac Automaticity of m/hESC-CMs during Differentiation

We next investigated if I_{K1} -induced I_f activation plays a role in regulating cardiac automaticity and studied the EP properties of m/hESC-differentiated CMs (Table 1). Around half of m/hESC-CMs could spontaneously fire APs, including ventricular and atrial CMs, with the remaining being quiescent-yet-excitabile (Fig. 3a-b). We found that the maximum diastolic potential (MDP) of spontaneously-firing ESC-CMs was significantly more hyperpolarized than that of quiescent cells, which, upon electrical pacing, could elicit an AP with a phase 4-like depolarization but failed to elicit subsequent APs. The MDP of quiescent-yet-excitabile atrial and ventricular mESC-CMs were -64.8 ± 2.1 mV ($n = 19$) and -67.5 ± 3.2 mV ($n = 13$), respectively; while the MDP was more hyperpolarized in spontaneously-firing atrial (-71.5 ± 1.5 mV, $n = 13$, $p = 0.002$) and ventricular (-72.4 ± 3.1 mV, $n = 12$, $p = 0.026$) mESC-CMs (Fig. 3c). The same was also true for hESC-CMs (Fig. 3d and Table 1). We also performed single cell qRT-PCR and confirmed that cells that elicited APs in our patch-clamp recording were all CMs with high expression of cardiac sarcomere genes (i.e. *TNNT2*, *MYH6*, *MYL7*, *MYL3*) and cardiac ion channels (Fig. 3e). The mRNA expressions of ion channels varied among individual ESC-CMs and had no significant difference between quiescent-yet-excitabile and spontaneously-firing cells. We found that *HCN4* and *KCNJ2* (*Kir2.1*) were the major channels mediating I_{K1} and I_f in hESC-CMs. Consistently, our immunocytochemistry staining confirmed that both *HCN4* and *Kir2.1* were expressed in hESC-CMs, which had formed typical sarcomere structure (Fig. 3f).

We then measured functional currents of I_{K1} and I_f and found that a low amount of I_{K1} could be measured only in ventricular mESC-CMs (Fig. 4a) and hESC-CMs [23], while I_f was recorded in all m/hESC-CMs. We found that a bigger I_f was measured in quiescent cells than in spontaneously-firing mESC-CMs (Fig. 4b), but the stable activation curves of I_f in both types of cells had no difference (Fig. 4c). However, spontaneously-firing ventricular mESC-CMs ($n = 4$) had a relatively bigger outward current of I_{K1} than quiescent-yet-excitabile ventricular cells ($n = 5$, $p = 0.04$, Fig. 4d), which might be the cause of a relatively positive MDP in quiescent m/hESC-CMs.

Rather than classical depolarization pacing, we applied a modest outward current to mimic I_{K1} for hyperpolarizing the MP and investigated whether the low automaticity of quiescent ESC-CMs is caused by the relatively positive MDP. Upon injection of a 30pA outward current, interestingly, the quiescent-yet-excitabile mESC-CMs fired APs spontaneously ($n = 5$) (Fig. 4e). We also treated hESC-CMs with zacopride, which could specifically enhance I_{K1} in isolated rat CMs without influence on other ion currents [38], to study if the automaticity can be developed in quiescent-yet-excitabile ESC-CMs by an increased I_{K1} , after we validated that zacopride (10 μ Mol/L) had no influence on I_f (Fig. S3). We found that zacopride could induce automaticity in quiescent-yet-excitabile hESC-CMs (6 out of 8 cells) to spontaneously fire APs (Fig. 4f). Our results demonstrated that an increased I_{K1} could enhance the automaticity of m/hESC-CMs and hyperpolarization of MP is important for the development of cardiac automaticity.

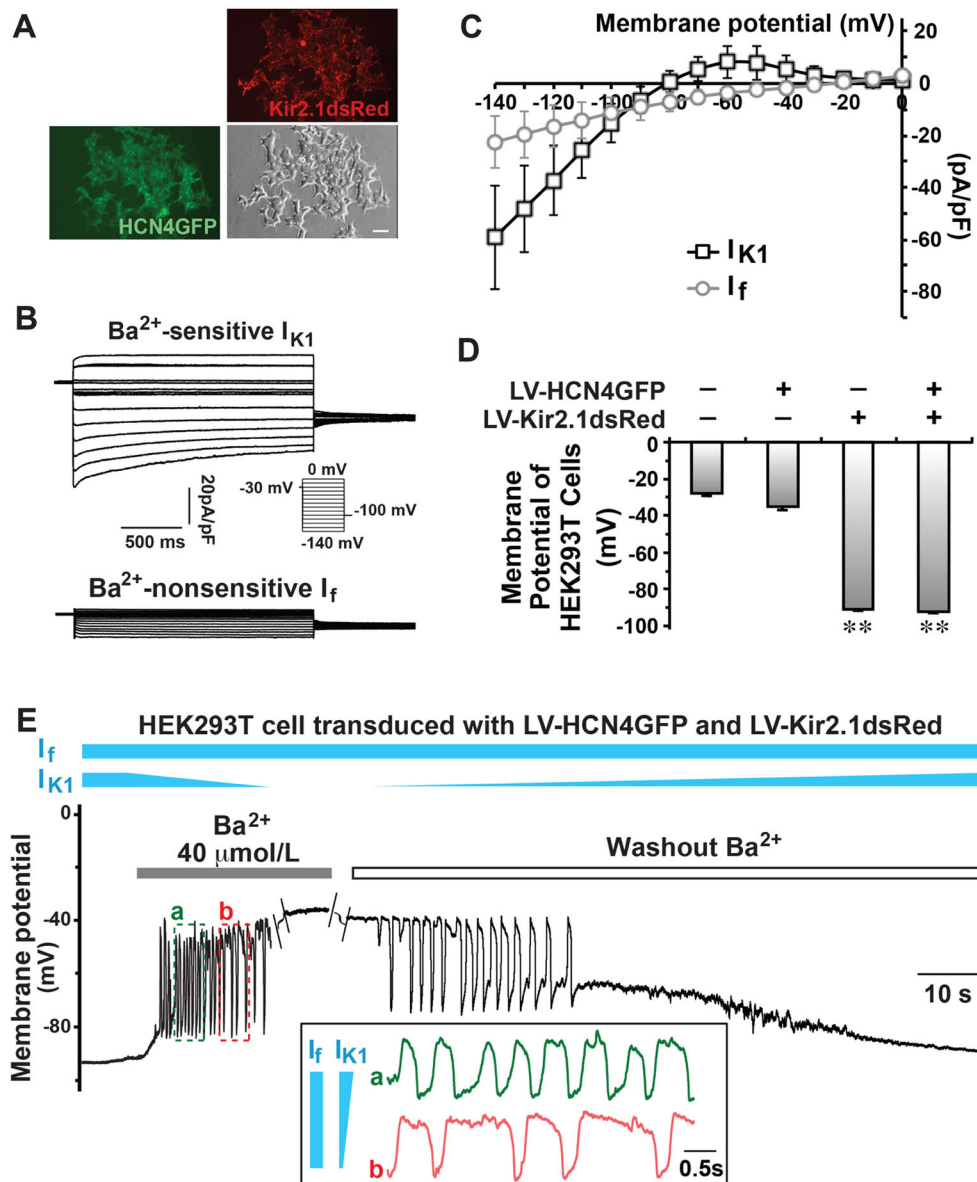


Fig. 2 Pacemaker-like rhythmic oscillations of MP could be generated by I_{K1} and I_f in bioengineered HEK293T cells. **a** Two fusion proteins, HCN4GFP and Kir2.1dsRed, were introduced into HEK293T cells by lentivirus infection. A bar indicates 20 μm . **b** Representative I_{K1} and I_f were recorded in bioengineered HEK293T cells. **c** I-V curves of I_{K1} and I_f in bioengineered Kir2.1dsRed/HCN4GFP HEK293T cells. **d** The RMP of HEK293T cells with/without infection. ****** $p < 0.01$ vs. non-infected

cells. **e** The oscillation of MP was recorded by patch clamp in a bioengineered HEK293T cell co-transduced with LV-HCN4GFP and LV-Kir2.1dsRed, when I_{K1} was partially inhibited by Ba^{2+} . The inset panel compared the oscillations at two different time points (**a** and **b**), showing that an increased I_{K1} could enhance the firing rate of oscillations

Acute Upregulation of I_f Inhibited the Automaticity of m/hESC-CMs

Since CMs differentiated from a stable transgenic cell line of mESCs overexpressing HCN4 showed significantly more rapid beating capability [31], we also investigated if bio-engineered pacemaker cells could be developed from differentiated ESC-CMs by an acute upregulation of I_f . We infected hESC-CMs with

adenovirus of Ad-CGI-HCN, which was used to convert quiescent adult ventricular CMs into spontaneously-firing pacemaker-like cells [10, 34]. Ad-CGI-HCN infection significantly increased I_f in hESC-CMs (Fig. 5a-b). We found that I_f upregulation had no significant effect on changing atrial or ventricular cell types of hESC-CMs (Fig. 5c). However, the percentage of spontaneously-firing hESC-CMs was significantly decreased from 45.5% in the control ($n = 33$) to 28.5%

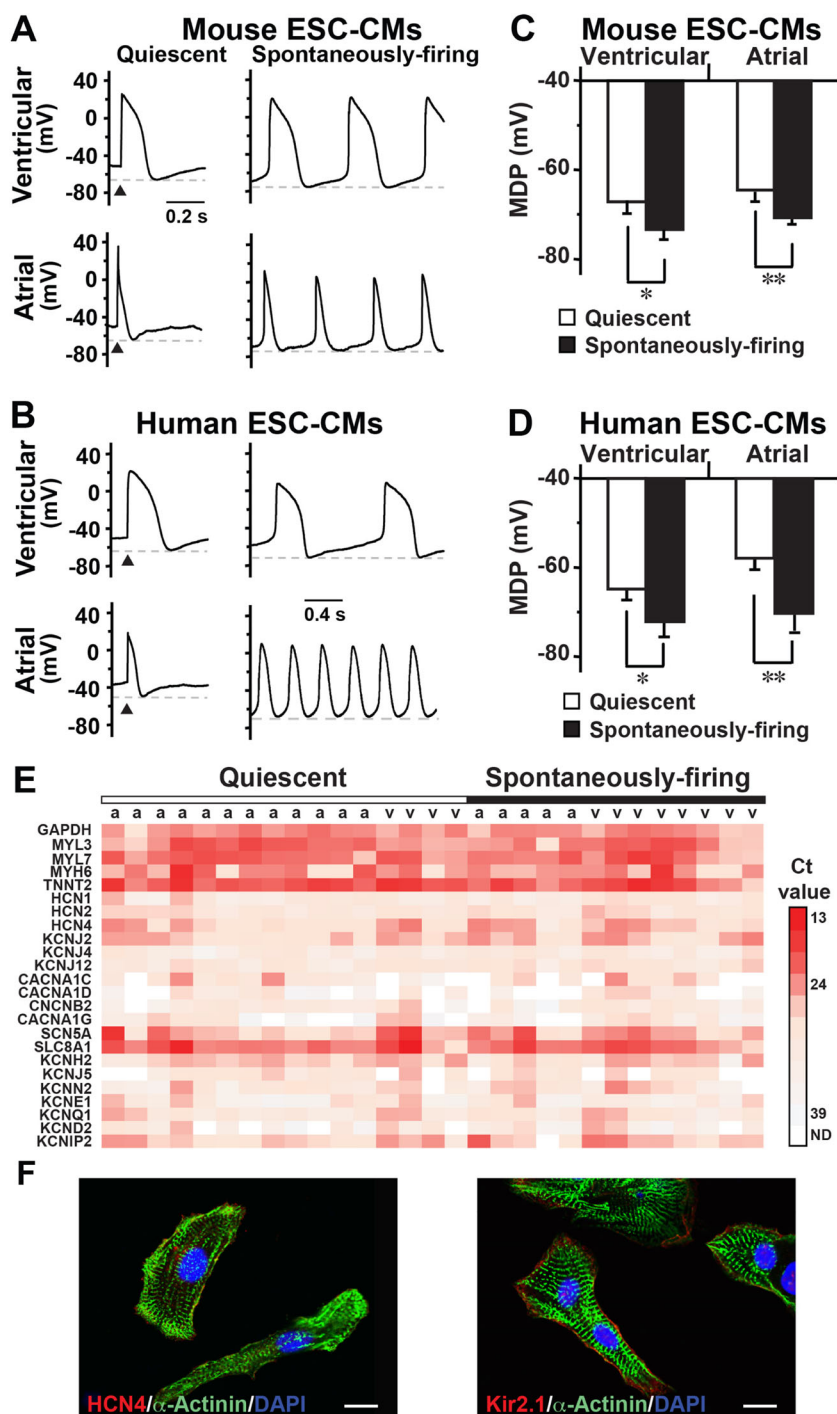


Fig. 3 Spontaneously-firing m/hESC-CMs had a more hyperpolarized maximum diastolic potential (MDP). **a–b** Representative APs of quiescent and spontaneously-firing mouse (**a**) and human (**b**) ESC-CMs. **c–d** The MDP of spontaneously-firing cells were significantly more hyperpolarized than that of quiescent cells in mouse (**c**) and human (**d**)

ESC-CMs. $*p < 0.05$, $**p < 0.01$. **e** A heat map of single cell qRT-PCR shows gene expression in individual atrial (**a**) and ventricular (**v**) hESC-CMs of our patch-clamp recording. **f** Immunocytochemistry showed that hESC-CMs formed typical sarcomere structure and expressed HCN4 and Kir2.1. Bars indicate 10 μ m

($n = 28$, $p = 0.03$) in Ad-CGI-HCN cells (Fig. 5d). The spontaneously-firing rate of Ad-CGI-HCN-transduced ventricular hESC-CMs (34.5 ± 7.0 fpm, $n = 8$) had no significant difference than that in control cells

(35.7 ± 6.3 fpm, $n = 9$, Table 1). The same result was also observed in mESC-CMs. There was around 46.7% of control mESC-CMs ($n = 60$) that could spontaneously fire APs; however, most Ad-CGI-HCN–

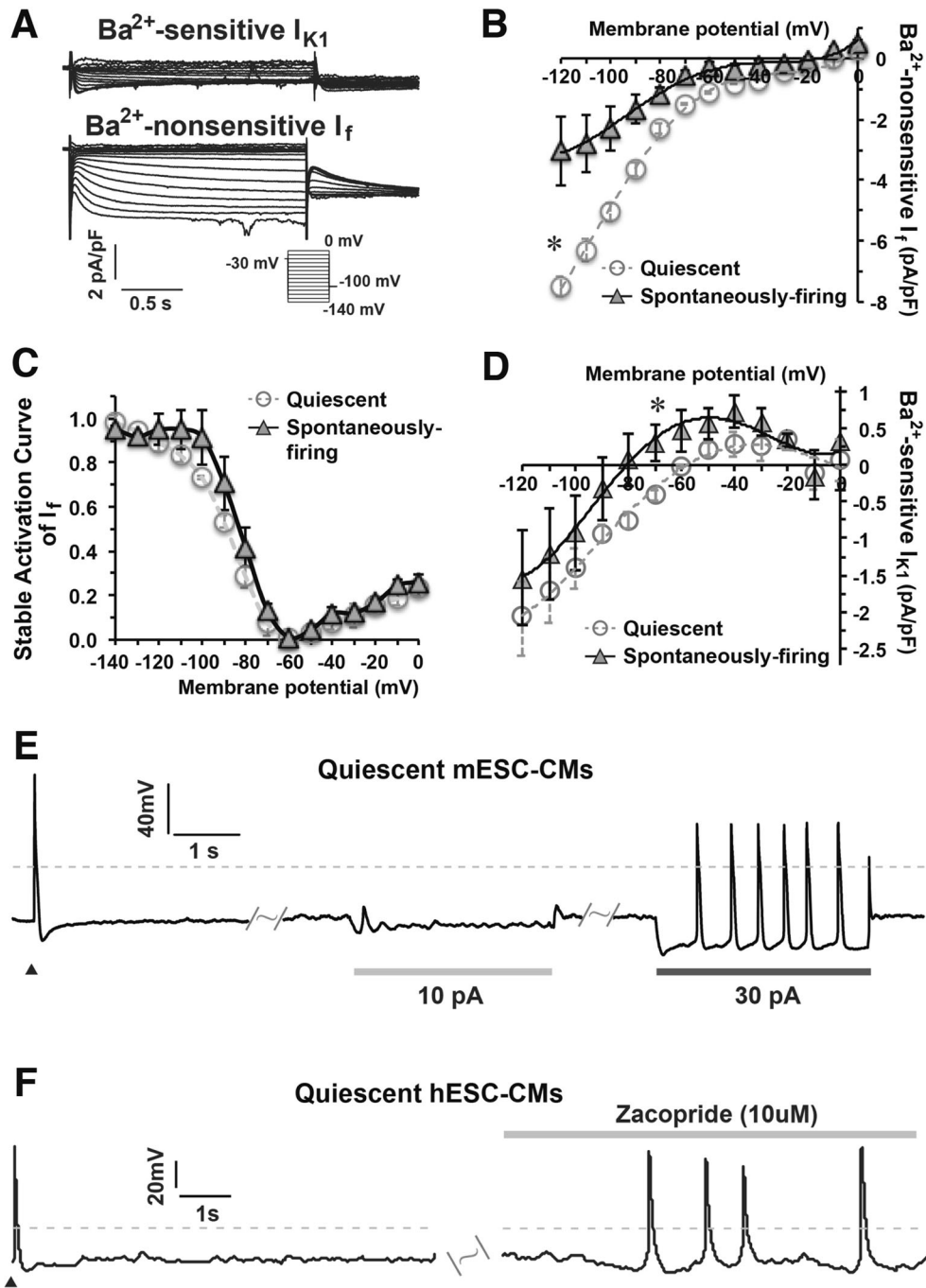


Fig. 4 A hyperpolarized MP enhanced the automaticity of quiescent m/hESC-CMs. **a** Representative I_{K1} and I_f were recorded in ventricular mESC-CMs. **b-c** The I-V curve and stable activation curve of I_f in quiescent ($n = 5$) and spontaneously-firing ($n = 4$) ventricular mESC-CMs. **d** The I-V curve of I_{K1} showing that spontaneously-firing ventricular mESC-CMs ($n = 4$) displayed a bigger outward current of I_{K1} than

quiescent-yet-excitable ventricular mESC-CMs ($n = 5$). **e** Quiescent mESC-CMs ($n = 5$) could spontaneously elicit APs when a proper amount of electrode-injected outward current hyperpolarized the MP. **f** The automaticity of quiescent hESC-CMs (6 out of 8, right) was enhanced to fire APs spontaneously after zacopride treatment. Dash lines indicate 0 mV, \blacktriangle indicates an electrical stimulation

transduced mESC-CMs became quiescent-yet-excitable and only 10.1% of them ($n = 69$, $p = 0.01$) could fire APs spontaneously (Fig. 5e) without enhancement of the firing rate (Table 1). These experiments demonstrated that acute upregulation of I_f inhibited the automaticity of m/hESC-CMs.

Discussion

In this study, we investigated a synergistic interaction of I_{K1} and I_f that regulates cardiac automaticity and found that I_{K1} -induced I_f activation could generate pacemaker-like rhythmic oscillation of MP even in otherwise unexcitable cells. We

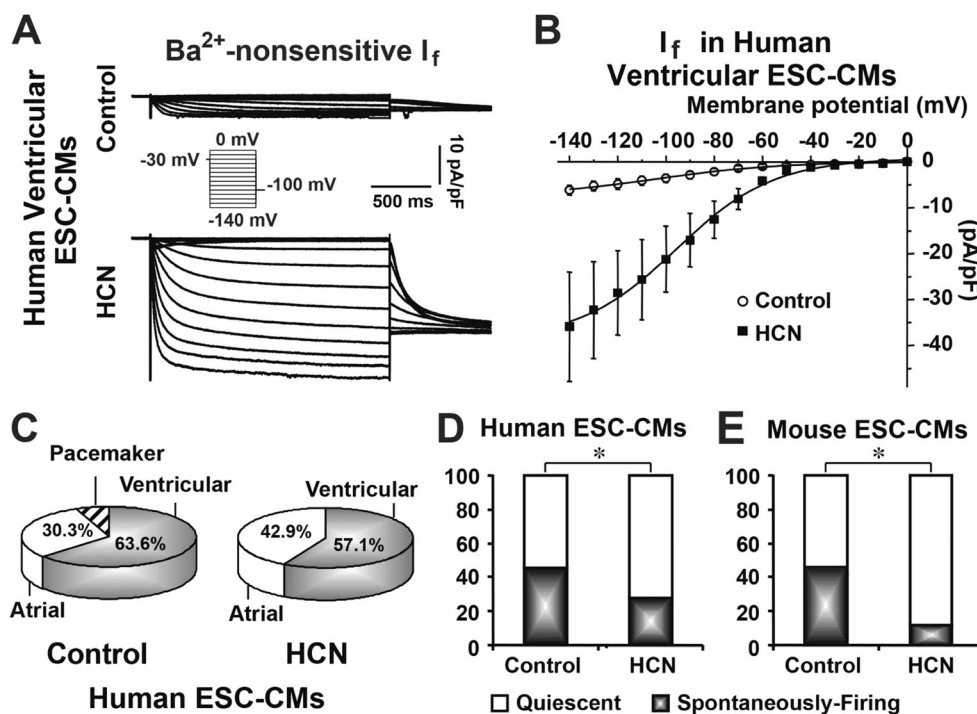


Fig. 5 Acute upregulation of I_f suppressed the automaticity of m/hESC-CMs. **a** Representative traces of I_f recorded in Ad-CGI- (control) and Ad-CGI-HCN-transduced (HCN) ventricular hESC-CMs. **b** The I-V curves of I_f in control and HCN-ventricular hESC-CMs. **c** Acute upregulation of

I_f didn't change chamber-specific cell types of hESC-CMs. **d-e** Acute upregulated I_f significantly decreased the number of spontaneously-firing cells in human (**d**) and mouse (**e**) ESC-CMs. * $p < 0.05$

found that I_{K1} and I_f could influence each other in enhancing or suppressing cardiac automaticity. A small amount of increased I_{K1} could improve the development of cardiac automaticity in m/hESC-CMs through a mechanism of I_{K1} -induced I_f activation, which is a singular role of I_{K1} in regulating cardiac automaticity. We also found that acute upregulation of I_f surprisingly suppressed cardiac automaticity of m/hESC-CMs in which a low amount of I_{K1} was measured. Our study advances the conventional view of I_{K1} in regulating cardiac automaticity of spontaneously-firing APs.

As opposed to the dynamic nature of spontaneously-firing cells, the RMP of quiescent cells is highly stable until they get excited and is mostly determined by the concentrations and conductance of different ions across the membrane. Undifferentiated cells show highly variable RMP, which is usually significantly more positive than that of differentiated cells [39]. In our recordings, the RMP was around -30 mV in unexcitable HEK293T cells (Fig. 3c) and -15 mV in undifferentiated mESCs. The normal RMP of adult ventricular CMs is hyperpolarized to -90 mV, mostly due to a constant outward leak of I_{K1} potassium current through inward rectifier channels [14, 29]. Therefore, the RMP is being gradually hyperpolarized during the differentiation and maturation of CMs. The development of sarcolemmal I_f plays a major role to initiate a sarcolemmal electrical automaticity of firing APs [5–7], which was found being developed earlier than cell contraction during CM-differentiation in chicken embryos [40,

41]. By definition, the activation of I_f requires a hyperpolarized MP; therefore, hyperpolarization of RMP during CM differentiation is indeed critical for the ultimate development of automaticity in differentiated muscle cells. It has been found that MP hyperpolarization by I_{K1} is critical for skeletal muscle differentiation from human myoblasts [42]. Consistently, our EP studies found that spontaneously-firing m/hESC-CMs displayed more hyperpolarized MDP than quiescent ESC-CMs (Fig. 4), in which automaticity was enhanced to fire APs spontaneously by an I_{K1} -specific agonist zacopride or an electrode-injected outward current. Therefore, we speculate that quiescent m/hESC-CMs might be less differentiated at an intermediate differentiation stage between spontaneously-firing ESC-CMs and cardiac progenitor/precursor cells. The presence of a small amount of I_{K1} hyperpolarizes RMP and plays a critical role in developing cardiac automaticity in newly-differentiated CMs through a mechanism I_{K1} -induced I_f activation. During the later maturation process, a further increased I_{K1} together with a decreased I_f suppresses cardiac automaticity in adult ventricular and atrial CMs.

Another possibility that could explain less I_{K1} measured in quiescent m/hESC-CMs is the vulnerability of I_{K1} to cell isolation methods [43], which could cause a decreased I_{K1} in some m/hESC-CMs and consequently led to a suppressed automaticity. However, this explanation also suggests a novel role of I_{K1} in enhancing cardiac automaticity. Indeed, in contrast to the increased beating frequency of ventricular

myocytes, a consistently slower sinus-paced rhythmic heart rate in the Kir2.1-knockout mice [18] may also indicate the possibility that I_{K1} has a critical role of enhancing cardiac automaticity.

The mechanism of I_{K1} -induced I_f activation is consistent with previous studies of developing biological pacemakers. The amount and ratio of I_{K1} and I_f is critical to eliciting rhythmic electrical activity. Normally, adult cardiac ventricular muscle cells have a large amount of I_{K1} and a low level of I_f ; therefore, both strategies of down-regulating I_{K1} [29] and up-regulating I_f [9, 10] in ventricular CMs could successfully develop bio-engineered pacemaker cells to spontaneously fire APs. Saito et al. established a transgenic cell line of mouse ESCs stably overexpressing HCN4GFP and found that CMs differentiated from HCN4GFP-transgenic mESCs displayed an enhanced automaticity [31]. Although they didn't categorize mESC-CMs into chamber-specific cell types for the comparison of automaticity, this study still inspired us to develop bio-pacemaker cells from m/hESC-CMs. Unfortunately, acute upregulation of I_f actually suppressed cardiac automaticity in m/hESC-CMs, which was also observed in atrial CMs [44]. Although it is unknown if a constant overexpression of HCN4 in previous study [31] or acute overexpression of HCN4 in our current study would influence the expression of immaturity markers in m/hESC-CMs, our study demonstrates that m/hESC-CMs couldn't be directly converted into bio-pacemaker cells by acute-upregulation of I_f .

It has been noticed that different ESC lines have distinct cardiogenic preferences [45] and the culturing and differentiation methods of ESCs have a big impact the efficiency and cardiac lineages of CM-differentiation [46], which might possibly influence the expression of cardiac ion channels and subsequently affect the development of cardiac automaticity. This might be an important concern for induced pluripotent stem cells (iPSCs), which remain an epigenetic memory of the donor cell source [47]. In our study, we found that I_{K1} -induced I_f activation could regulate the automaticity of mouse and human ESC-CMs differentiated with two different methods, EB-differentiation and inductive co-culture, indicating a general role of I_{K1} -induced I_f activation during the development of cardiac automaticity. This is consistent with previous finding that the epigenetic memory of cardiac somatic cell source does not influence the functional outcome of iPSC-differentiated CMs, while it improves cardiac differentiation efficiency [48].

One limitation is that our current study focused on regulating cellular automaticity by the sarcolemmal currents of I_{K1} -induced I_f activation but didn't include the influence of intracellular Ca^{2+} transients, which coordinates together with sarcolemmal ion currents to control cellular automaticity [49, 50]. Recently, Vaidyanathan et al. found that upregulated I_{K1} could enhance the amplitude of Ca^{2+} transients in iPSC-CMs [51]; therefore, the automaticity development promoted by

I_{K1} -induced I_f activation might be also mediated partially through intracellular Ca^{2+} transients. In addition, only Kir2.1 was utilized to study I_{K1} -induced I_f activation in bioengineered-HEK293T cells. It has been found that Kir2.1 is the major component of murine I_{K1} , but Kir2.2 also contribute to the native I_{K1} in mouse ventricular CMs [18]. Therefore, It is possible that both Kir2.1 and Kir2.2, or even Kir2.3, contribute to the development of cardiac automaticity in m/hESC-CMs.

In conclusion, our study explored the synergistic interaction between I_{K1} and I_f and revealed a singular role of I_{K1} in the ultimate development of cardiac automaticity in m/hESC-CMs by I_{K1} -induced I_f activation. Our study provides a more comprehensive understanding of I_{K1} regulating cardiac automaticity, which will guide us to investigate the role of I_{K1} in arrhythmogenesis and develop efficient strategies for anti-arrhythmic therapy.

Acknowledgments We are grateful to Dr. Jill Dunham for editorial assistance. This work was supported by the Start-up Fund from The MetroHealth System (to J.D.F.) and grants from the American Heart Association-13SDG14580035 (to J.D.F.), the Research Grant Council (TRS T13-706/11 to R.A.L.) and the National Institutes of Health (NIH)-R01HL096962 (to I.D.), NIH-R21HL123012 (to K.R.L.).

Compliance with Ethical Standards

Disclosures No disclosure of conflict interest.

References

- Christoffels, V. M., Smits, G. J., Kispert, A., & Moorman, A. F. (2010). Development of the pacemaker tissues of the heart. *Circulation Research*, *106*, 240–254.
- Mangoni, M. E., & Nargeot, J. (2008). Genesis and regulation of the heart automaticity. *Physiological Reviews*, *88*, 919–982.
- Wilders, R. (2007). Computer modelling of the sinoatrial node. *Medical & Biological Engineering & Computing*, *45*, 189–207.
- Ludwig, A., Zong, X., Jeglitsch, M., Hofmann, F., & Biel, M. (1998). A family of hyperpolarization-activated mammalian cation channels. *Nature*, *393*, 587–591.
- DiFrancesco, D., & Noble, D. (2012). The funny current has a major pacemaking role in the sinus node. *Heart Rhythm*, *9*, 299–301.
- DiFrancesco, D. (2010). The role of the funny current in pacemaker activity. *Circulation Research*, *106*, 434–446.
- Cohen, I. S., & Robinson, R. B. (2006). Pacemaker current and automatic rhythms: Toward a molecular understanding. *Handbook of Experimental Pharmacology*, 41–71.
- Qu, J., Barbuti, A., Protas, L., Santoro, B., Cohen, I. S., & Robinson, R. B. (2001). HCN2 overexpression in newborn and adult ventricular myocytes: Distinct effects on gating and excitability. *Circulation Research*, *89*, E8–14.
- Qu, J., Plotnikov, A. N., Danilo Jr., P., et al. (2003). Expression and function of a biological pacemaker in canine heart. *Circulation*, *107*, 1106–1109.
- Tse, H. F., Xue, T., Lau, C. P., et al. (2006). Bioartificial sinus node constructed via in vivo gene transfer of an engineered pacemaker

- HCN Channel reduces the dependence on electronic pacemaker in a sick-sinus syndrome model. *Circulation*, *114*, 1000–1011.
11. Kubo, Y., Baldwin, T. J., Jan, Y. N., & Jan, L. Y. (1993). Primary structure and functional expression of a mouse inward rectifier potassium channel. *Nature*, *362*, 127–133.
 12. Tourneur, Y., Mitra, R., Morad, M., & Rougier, O. (1987). Activation properties of the inward-rectifying potassium channel on mammalian heart cells. *The Journal of Membrane Biology*, *97*, 127–135.
 13. Ibarra, J., Morley, G. E., & Delmar, M. (1991). Dynamics of the inward rectifier K⁺ current during the action potential of guinea pig ventricular myocytes. *Biophysical Journal*, *60*, 1534–1539.
 14. Miake, J., Marban, E., & Nuss, H. B. (2003). Functional role of inward rectifier current in heart probed by Kir2.1 overexpression and dominant-negative suppression. *The Journal of Clinical Investigation*, *111*, 1529–1536.
 15. Shinagawa, Y., Satoh, H., & Noma, A. (2000). The sustained inward current and inward rectifier K⁺ current in pacemaker cells dissociated from rat sinoatrial node. *The Journal of Physiology*, *523*(Pt 3), 593–605.
 16. Cho, H. S., Takano, M., & Noma, A. (2003). The electrophysiological properties of spontaneously beating pacemaker cells isolated from mouse sinoatrial node. *The Journal of Physiology*, *550*, 169–180.
 17. Guo, J., Mitsuiye, T., & Noma, A. (1997). The sustained inward current in sino-atrial node cells of guinea-pig heart. *Pflügers Archiv*, *433*, 390–396.
 18. Zaritsky, J. J., Redell, J. B., Tempel, B. L., & Schwarz, T. L. (2001). The consequences of disrupting cardiac inwardly rectifying K(+) current (IK1) as revealed by the targeted deletion of the murine Kir2.1 and Kir2.2 genes. *The Journal of Physiology*, *533*, 697–710.
 19. Plaster, N. M., Tawil, R., Tristani-Firouzi, M., et al. (2001). Mutations in Kir2.1 cause the developmental and episodic electrical phenotypes of Andersen's syndrome. *Cell*, *105*, 511–519.
 20. Liu, A., Tang, M., Xi, J., et al. (2010). Functional characterization of inward rectifier potassium ion channel in murine fetal ventricular cardiomyocytes. *Cellular Physiology and Biochemistry: International Journal of Experimental Cellular Physiology, Biochemistry, and Pharmacology*, *26*, 413–420.
 21. Masuda, H., & Sperelakis, N. (1993). Inwardly rectifying potassium current in rat fetal and neonatal ventricular cardiomyocytes. *The American Journal of Physiology*, *265*, H1107–H1111.
 22. Fu, J. D., Jiang, P., Rushing, S., Liu, J., Chiamvimonvat, N., & Li, R. A. (2010). Na⁺/Ca²⁺ exchanger is a determinant of excitation-contraction coupling in human embryonic stem cell-derived ventricular cardiomyocytes. *Stem Cells and Development*, *19*, 773–782.
 23. Lieu, D. K., Fu, J. D., Chiamvimonvat, N., et al. (2013). Mechanism-based facilitated maturation of human pluripotent stem cell-derived cardiomyocytes. *Circulation. Arrhythmia and Electrophysiology*, *6*, 191–201.
 24. Fu, J. D., Rushing, S. N., Lieu, D. K., et al. (2011). Distinct roles of microRNA-1 and -499 in ventricular specification and functional maturation of human embryonic stem cell-derived cardiomyocytes. *PLoS One*, *6*, e27417.
 25. Kehat, I., Kenyagin-Karsenti, D., Snir, M., et al. (2001). Human embryonic stem cells can differentiate into myocytes with structural and functional properties of cardiomyocytes. *The Journal of Clinical Investigation*, *108*, 407–414.
 26. Mummery, C., Ward-van Oostwaard, D., Doevendans, P., et al. (2003). Differentiation of human embryonic stem cells to cardiomyocytes: Role of coculture with visceral endoderm-like cells. *Circulation*, *107*, 2733–2740.
 27. Xue, T., Cho, H. C., Akar, F. G., et al. (2005). Functional integration of electrically active cardiac derivatives from genetically engineered human embryonic stem cells with quiescent recipient ventricular cardiomyocytes: Insights into the development of cell-based pacemakers. *Circulation*, *111*, 11–20.
 28. He, J. Q., Ma, Y., Lee, Y., Thomson, J. A., & Kamp, T. J. (2003). Human embryonic stem cells develop into multiple types of cardiac myocytes: Action potential characterization. *Circulation Research*, *93*, 32–39.
 29. Miake, J., Marban, E., & Nuss, H. B. (2002). Biological pacemaker created by gene transfer. *Nature*, *419*, 132–133.
 30. Chan, Y. C., Siu, C. W., Lau, Y. M., Lau, C. P., Li, R. A., & Tse, H. F. (2009). Synergistic effects of inward rectifier (I) and pacemaker (I) currents on the induction of bioengineered cardiac automaticity. *Journal of Cardiovascular Electrophysiology*, *20*, 1048–1054.
 31. Saito, Y., Nakamura, K., Yoshida, M., et al. (2015). Enhancement of spontaneous activity by HCN4 overexpression in mouse embryonic stem cell-derived Cardiomyocytes - a possible biological pacemaker. *PLoS One*, *10*, e0138193.
 32. Wobus, A. M., Guan, K., Yang, H. T., & Boheler, K. R. (2002). Embryonic stem cells as a model to study cardiac, skeletal muscle, and vascular smooth muscle cell differentiation. *Methods in Molecular Biology*, *185*, 127–156.
 33. Reubinoff, B. E., Pera, M. F., Fong, C. Y., Trounson, A., & Bongso, A. (2000). Embryonic stem cell lines from human blastocysts: Somatic differentiation in vitro. *Nature Biotechnology*, *18*, 399–404.
 34. Xue, T., Siu, C. W., Lieu, D. K., Lau, C. P., Tse, H. F., & Li, R. A. (2007). Mechanistic role of I(f) revealed by induction of ventricular automaticity by somatic gene transfer of gating-engineered pacemaker (HCN) channels. *Circulation*, *115*, 1839–1850.
 35. Wang, K., Xue, T., Tsang, S. Y., et al. (2005). Electrophysiological properties of pluripotent human and mouse embryonic stem cells. *Stem Cells*, *23*, 1526–1534.
 36. Ma, J., Guo, L., Fiene, S. J., et al. (2011). High purity human-induced pluripotent stem cell-derived cardiomyocytes: Electrophysiological properties of action potentials and ionic currents. *American Journal of Physiology. Heart and Circulatory Physiology*, *301*, H2006–H2017.
 37. Dokos, S., Celler, B., & Lovell, N. (1996). Ion currents underlying sinoatrial node pacemaker activity: A new single cell mathematical model. *Journal of Theoretical Biology*, *181*, 245–272.
 38. Liu, Q. H., Li, X. L., Xu, Y. W., Lin, Y. Y., Cao, J. M., & Wu, B. W. (2012). A novel discovery of IK1 channel agonist: Zacopride selectively enhances IK1 current and suppresses triggered arrhythmias in the rat. *Journal of Cardiovascular Pharmacology*, *59*, 37–48.
 39. Johnson, M. A., Weick, J. P., Pearce, R. A., & Zhang, S. C. (2007). Functional neural development from human embryonic stem cells: Accelerated synaptic activity via astrocyte coculture. *The Journal of Neuroscience: The Official Journal of the Society for Neuroscience*, *27*, 3069–3077.
 40. Kamino, K., Hirota, A., & Fujii, S. (1981). Localization of pacemaker activity in early embryonic heart monitored using voltage-sensitive dye. *Nature*, *290*, 595–597.
 41. Van Mierop, L. H. (1967). Location of pacemaker in chick embryo heart at the time of initiation of heartbeat. *The American Journal of Physiology*, *212*, 407–415.
 42. Konig, S., Hinard, V., Armaudeau, S., et al. (2004). Membrane hyperpolarization triggers myogenin and myocyte enhancer factor-2 expression during human myoblast differentiation. *The Journal of Biological Chemistry*, *279*, 28187–28196.
 43. Hoshino, S., Omatsu-Kanbe, M., Nakagawa, M., & Matsuura, H. (2012). Postnatal developmental decline in IK1 in mouse ventricular myocytes isolated by the Langendorff perfusion method: Comparison with the chunk method. *Pflügers Archiv*, *463*, 649–668.
 44. Lieu, D. K., Chan, Y. C., Lau, C. P., Tse, H. F., Siu, C. W., & Li, R. A. (2008). Overexpression of HCN-encoded pacemaker current silences bioartificial pacemakers. *Heart Rhythm*, *5*, 1310–1317.

45. Moore, J. C., Fu, J., Chan, Y. C., et al. (2008). Distinct cardiogenic preferences of two human embryonic stem cell (hESC) lines are imprinted in their proteomes in the pluripotent state. *Biochemical and Biophysical Research Communications*, *372*, 553–558.
46. Mummery, C. L., Zhang, J., Ng, E. S., Elliott, D. A., Elefanty, A. G., & Kamp, T. J. (2012). Differentiation of human embryonic stem cells and induced pluripotent stem cells to cardiomyocytes: A methods overview. *Circulation Research*, *111*, 344–358.
47. Kim, K., Doi, A., Wen, B., et al. (2010). Epigenetic memory in induced pluripotent stem cells. *Nature*, *467*, 285–290.
48. Sanchez-Freire, V., Lee, A. S., Hu, S., et al. (2014). Effect of human donor cell source on differentiation and function of cardiac induced pluripotent stem cells. *Journal of the American College of Cardiology*, *64*, 436–448.
49. Lakatta, E. G., Maltsev, V. A., & Vinogradova, T. M. (2010). A coupled SYSTEM of intracellular Ca²⁺ clocks and surface membrane voltage clocks controls the timekeeping mechanism of the heart's pacemaker. *Circulation Research*, *106*, 659–673.
50. Yaniv, Y., Lakatta, E. G., & Maltsev, V. A. (2015). From two competing oscillators to one coupled-clock pacemaker cell system. *Frontiers in Physiology*, *6*, 28.
51. Vaidyanathan, R., Markandeya, Y. S., Kamp, T. J., Makielski, J. C., January, C. T., & Eckhardt, L. L. (2016). IK1-enhanced human-induced pluripotent stem cell-derived cardiomyocytes: An improved cardiomyocyte model to investigate inherited arrhythmia syndromes. *American Journal of Physiology. Heart and Circulatory Physiology*, *310*, H1611–H1621.